High-power passively Q-switched thulium fiber laser with distributed stimulated Brillouin scattering

Tang, Yulong; Li, Xiaohui; Wang, Qi Jie

2013

High-power passively *Q*-switched thulium fiber laser with distributed stimulated Brillouin scattering

Yulong Tang,[1,2] Xiaohui Li,[1] and Qi Jie Wang[1,3,*]

[1]*OPTIMUS, Photonics Centre of Excellence, School of Electrical and Electronic Engineering, Nanyang Technological University, 50 Nanyang Avenue, Singapore 639798*

[2]*Key Laboratory for Laser Plasmas (Ministry of Education) and Department of Physics and Astronomy, Shanghai Jiao Tong University, Shanghai 200240, China*

[3]*CDPT, Centre for Disruptive Photonic Technologies, Nanyang Technological University, Singapore 637371*
*Corresponding author: qjwang@ntu.edu.sg

We report a novel passively *Q*-switched 2 μm Tm^{3+} fiber laser simply by distributed stimulated Brillouin scattering with an all-fiber configuration. The maximum output power is 2.49 W with an optical-to-optical slope efficiency of 12%, and the laser wavelength is centered at ~1991 nm with a spectral width of >10 nm. The single pulse energy can be over 50 μJ with a pulse width of about 20 ns, and the pulse repetition rate can be tuned from several kilohertz to tens of kilohertz by changing the pump power. To the best of our knowledge, this is the highest-average-power passively *Q*-switched 2 μm Tm^{3+} fiber laser in the nanosecond regime.   © 2012 Optical Society of America

OCIS codes: (140.3510) Lasers, fiber; (140.3540) Lasers, Q-switched; (060.3510) Lasers, fiber; (060.2320) Fiber optics amplifiers and oscillators.
http://dx.doi.org/10.1364/OL.38.005474

In recent years, Tm^{3+}-doped fiber lasers (TDFLs) at 2 μm have stimulated increasing research interest due to the fact that the 2 μm spectral range covers the heavy absorption peak of water molecules. Being named "eye-safe" lasers, TDFL shave found wide applications in remote sensing, LIDAR, industrial machining, frequency conversion, and biomedicine [1–3]. However, some applications require high peak power and high pulse energy 2 μm laser beams, which cannot be steadily obtained from TDFLs, owing to the lack of high-power modulation elements in this wavelength region. Whereas, continuous wave (CW) mode ~2 μm TDFLs have achieved >1 kW power [4], pulsed-mode counterparts still need further development to meet various application requirements.

Pulsed 2 μm TDFLs are generally constructed using *Q*-switching [5,6] or mode-locking [7,8], but the laser power and pulse energy are usually limited by damage to modulation elements or fiber facets. Acousto-optic *Q*-switched 2 μm TDFLs based on high pump ratios [9] or large-pitch fiber [10] have improved the average power to tens of watts, but the use of bulk modulators cannot provide an all-fiber configuration, decreasing system robustness. Gain-switched TDFLs have been proposed to generate high-energy [11,12] and high-average-power [13,14] 2 μm laser pulses, but these systems either possess spiky pulses (relaxation) or need a complex gain modulator. Resonant-pumped gain switching has realized stable pulsing operation [15], and high power also has been achieved through amplifying a gain seed [16]. However, it is difficult to achieve high average power from a passively modulated all-fiber oscillator with a pulse width of less than 50 ns.

To achieve high-power or high-energy 2 μm laser pulses, fiber-based master-oscillator-power-amplifier (MOPA) systems seeded by a regulated pulse appear to be attractive [17–20]. However, low seed power requires a large gain (e.g., >30 dB), thus a complicated multistage fiber amplifier structure [18–20], to scale the fiber laser to

a high power level. In this case, the large-mode-area fiber in the final stage amplifier for suppressing nonlinear effects and amplified stimulated emission (ASE) usually greatly decreases the output beam quality. On the contrary, if we have a high-power pulsed seed source, then the amplifier configuration will be greatly simplified (only one stage amplifier needed).

Previously, stimulated Brillouin scattering (SBS) has been used to narrow the pulse width in fiber lasers [21] and amplifiers [22], or to achieve passive *Q*-switching of fiber lasers [23–25]. However, regular pulsing operation can only be realized by employing a ring interferometer [24,25], and detailed pulsing characteristics were not reported.

In this Letter, we propose and realize a new technique to passively *Q*-switch 2 μm TDFLs with a simple configuration and high output power by making use of the distributed SBS feedback in a piece of ultrahigh numerical aperture (UHNA) fiber. This fiber laser provides the highest pulse energy and average power in passively modulated nanosecond fiber lasers (oscillators). Such high-power fiber lasers have a simple all-fiber structure, avoiding the use of complicated bulk modulators and isolators. The ~20 ns laser pulse is also the narrowest in passively *Q*-switched 2 μm fiber lasers, whose pulse-width narrowing is generally limited by long fiber length dictated by required high gain. This simple and efficient technique can be readily extended to other wavelength regions, such as 1, 1.5 μm and mid-infrared (3–5 μm).

Figure 1 depicts the schematic setup of the passively *Q*-switched TDFL. In order to achieve high average power, a double-cladding pumping technique was adopted. The double-clad Tm^{3+}-doped silica fiber (10/130 μm, 0.15/0.46 NA) had a Tm^{3+} doping concentration of ~2 wt.% and cladding absorption of ~3 dB/m (at 793 nm). The passive fiber is a 50 m length of UHNA fiber (Nufern Co., UHNA7), which has a core diameter of 3.5 μm with a NA of 0.41 and a clad diameter of 125 μm. A small
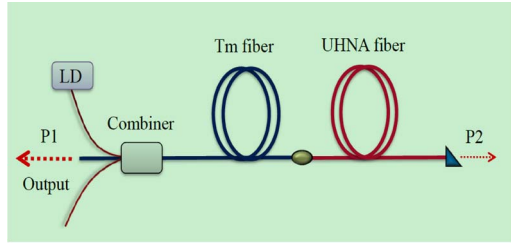
Fig. 1. Experimental setup of the passively Q-switched TDFL. LD: laser diode. Output from left-hand side is denoted as P1, and that from the right-hand side (the angle end of the UHNA fiber) is denoted as P2.

Fig. 2. Output of the Q-switched TDFL. Solid lines connected the data dots are for guiding the eye.

core area and large NA of this fiber provides strong light confinement (thus high light intensity) in the fiber core, facilitating nonlinear interaction between laser light and the fiber. The pump source was a 35 W 793 nm laser diode (LD) with a 100 μm (0.22 NA) pigtail fiber, and the pump light was launched into the Tm^{3+} fiber by using a $(2 + 1) \times 1$ fiber combiner, with a coupling efficiency of ~95%. One end of the UHNA fiber was fusion spliced to the Tm^{3+} fiber, and the other end of the UHNA fiber was ~10° angle cleaved. The signal fiber of the combiner (opposite to the end that connected to the Tm^{3+} fiber) was perpendicularly cleaved, providing a ~4% Fresnel feedback. With high pump power, high light intensity in the core of the UHNA fiber will stimulate Rayleigh scattering and SBS as a "random" distributed feedback [26]. This random distributed feedback combined with the ~4% Fresnel reflection from the left signal fiber end of the combiner complete the laser cavity. Output from the left-side signal fiber is denoted as P1 and that from the right-side UHNA fiber (angle-cleaved end) is dubbed as P2. The 5 m long Tm^{3+}-fiber was wrapped on a convectively cooled copper drum with a diameter of 10 cm. At the output end, a dichroic mirror ($R > 99.9\%$ at 793 nm, 0°) was used to filter residual pump light. The laser output power was measured with an OPHIR power meter (F150A-SH, OPHIR OPTRONICS LTD.), and the laser spectrum was recorded with a triple-grating spectrometer (Zolix Co.) with a spectral resolution of 0.2 nm. The laser pulsing dynamics were measured with a 500 MHz Agilent oscilloscope (DSO5054A) combined with an InGaAs detector.

Increasing the 793 nm pump power to 3.7 W, laser output P1 can be observed. Near threshold, the laser showed random pulsing, and the laser power had great fluctuations, as shown by the left dashed circle in Fig. 2 (we dub this the stability change point). Increasing the pump over 4.5 W, the pulsing operation went into the stable pulsing regime. In this case, the slope efficiency of P1 decreased because SBS has been stimulated, and this depleted most of the forwardly propagating laser light. Based on the equations in [27], the SBS threshold power is calculated to be ~0.16 W, which is very close to the 0.15 W P1 output at the 4.5 W pump level. In the stable region, the laser power P1 increases near linearly with pump, and the P2 also increases steadily. When the pump power is increased over 16.5 W, the slope of P1 drops slightly and P2 decreases. This is because that light intensity in the fiber core has surpassed the stimulated Raman scattering (SRS) threshold, and Raman scattering [Fig. 5(c)] depleted a fraction of the laser light. Based on
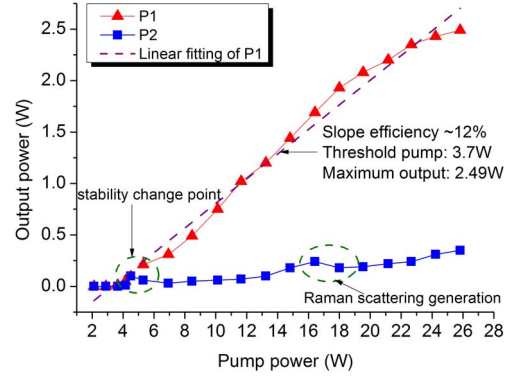
the equations in [27], the SRS threshold power is calculated to be ~120 W, which is close to the back-reflected intracavity laser peak power of 99 W (2.37 kW ÷ 0.96 × 4%) from the P1 end at the 16.5 W pump level. The maximum output power of P1 is 2.49 W, with a linear fitting slope efficiency of ~12% with respect to launched pump power. The maximum output power of P2 is 0.35 W, with 88% of the power being ~2 μm laser while 12% of the power being the Stokes (Raman emission) components (Fig. 5). The comparatively lower efficiency of the laser originated from low quality factor (weak feedback from both ends of the laser) of the cavity and high fusion loss between the Tm^{3+} fiber and the UHNA fiber. The maximum output power was mainly restricted by burning the coating of the UHNA fiber. Core pumping with Er-doped or Er/Yb-codoped fiber lasers, or employing a cladding-mode stripe, will effectively avoid coating burning. Better heat management in combination of higher pump power can further scale the average power.

The pulsing characteristics of the TDFL measured from P1 are shown in Fig. 3. The system has relatively high stability at moderate power levels (e.g., 1 W output). The relatively high stability resulted from certain optimization of the laser cavity. Too short passive fiber length, or adopting another kind of passive fiber (e.g., SMF28) with the same length as the SBS feedback element, will randomize the pulsing operation to some degree. Whereas the pulse train has a high temporal stability with a timing jitter of ~10%, the interpulse intensity fluctuation is about 20%. The stability decreases with increasing
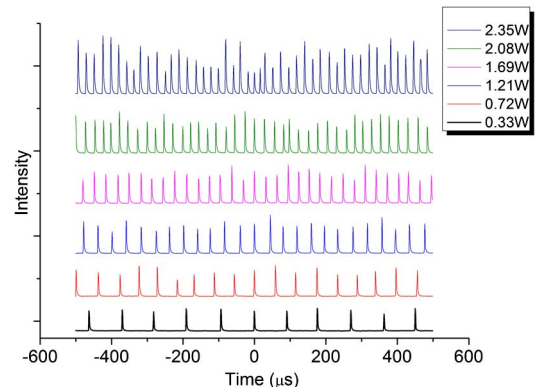

Fig. 3. Laser pulse train of the Q-switched TDFL at various average power levels of P1.

output power, partly owing to accumulated ASE and Raman scattering in the UHNA fiber, which also has influence on the slope efficiency. ASE and Raman scattering can be effectively suppressed by incorporating a narrow bandpass filter in the fiber laser. Therefore, this technique has great potential to become a stable and simple high-power Q-switching routine. In fact, our recent experiment has shown that the output power can be readily scaled to a higher power level (by several times) without any slope efficiency decrease.

Detailed evolution of pulsing characteristics [repetition rate (RR), pulse width, and peak power] of the Q-switched TDFL is shown in Fig. 4. The RR can be tuned from several kHz to over 50 kHz linearly increasing with pump power. Therefore, the RR of such fiber lasers can surpass that of conventional passively Q-switched fiber lasers, whose RR is usually restricted by fiber length. The peak power shows an irregular changing with pump, and the maximum peak power is 2.54 kW. At higher pump power, the peak power decreased owing to that part of the laser light was transferred to the Raman Stokes emission. Efficiently suppressing Raman scattering will not only improve the peak power but also the stability of the fiber laser at high power levels. The maximum pulse energy is ~53 μJ, which is much larger than those of passively Q-switched 2-μm fiber lasers [6,28] but still lower than those of positively gain switched fiber lasers [11,12].

Another intriguing point of this fiber laser is that its laser pulse width almost doesn't change with output power. This is a distinct property, which is different from that of conventional passively Q-switched fiber lasers, where the pulse narrows with increasing output power [29]. At all pump levels, the pulse width is clamped at ~20 ns, which is also the narrowest pulse width achieved in long (5 m) fiber lasers. In addition, the pulse shape did not depend on fiber length (Tm^{3+} fiber and UHNA fiber) at all.

The pulsing formation in this fiber laser can be attributed to distributed backscattering originated from SBS and Rayleigh scattering and is qualitatively explained as follows. At the beginning, the pump stimulates the Tm^{3+} fiber to build up population inversion. However, CW lasing is inhibited because reflection from the UHNA fiber-end facet is suppressed by the imposed angle (P2 end). With increasing pump, the ~4% Fresnel reflection from the P1 end fiber-facet and the backward feedback provided by the distributed Rayleigh scattering in the UHNA fiber can build up a low-quality-factor (half-random) cavity, which will greatly increase the laser intensity in the fiber. Linewidth narrows under the effect of Rayleigh scattering, and, consequently, the SBS threshold is reached. The backward SBS provides strong feedback in the form of a short SBS relaxation oscillation pulse. This pulse transits through the highly inverted Tm^{3+} fiber, experiencing high gain and extracting most of the stored energy. Consequently, a giant pulse comes out from the P1 fiber end. Reflection of this pulse from the P1 end fiber facet (~4% Fresnel reflection) will extract the remaining energy in the Tm^{3+} fiber, forming the output P2. The pulsing formation is mainly based on the SBS relaxation dynamics; leading to the pulse width has little to do with pump levels or fiber length. Assuming 10 MHz SBS bandwidth [30] in the UHNA fiber, the phonon decay time is calculated ($\cong 1/2\pi\Gamma_B$, where Γ_B is the SBS gain bandwidth) to be ~16 ns, which is close to our measured pulse width of ~20 ns.

The laser spectra measured at two power levels are shown in Fig. 5. At a comparatively lower output level (10 W pump), the spectrum shows multiple peaks, and the wavelength is centered at 1991 nm with a FWHM bandwidth of 16 nm, which is comparable to the high-power multimode Tm^{3+} fiber laser [31]. The broad bandwidth can be attributed to high gain in the single-mode fiber, as well as no mode selecting management employed (many longitudinal modes can obtain enough gain to overcome cavity loss). At a 16.4 W pump level, the FWHM is broadened to ~20 nm with a broad shoulder over 50 nm, which mainly originated from ASE and non-linear effects under high peak power (e.g., self-phase modulation, modulation instability). The signal-to-noise ratio (SNR) measured at 1.5 W output level was larger than 20 dB and decreased to ~15 dB at the maximum output level. Incorporating a band pass filter or saturable absorber element (e.g., Ho^{3+} fiber) into the fiber laser can suppress ASE, thus improve SNR. The center wavelength was mainly dictated by the gain peak of the Tm^{3+} fiber, and no obvious pump dependence of the center wavelength was observed. At the P2 port, the wavelength shifts to 1994 nm owing to laser reabsorption of the Tm^{3+} fiber. The bandwidth is narrowed to ~13 nm due the filtering effects of reabsorption and SBS. The Raman
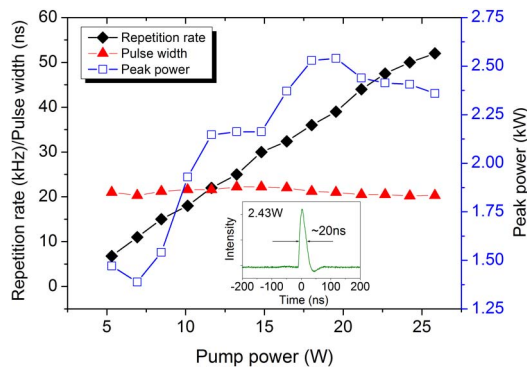
Fig. 4. Laser pulsing characteristics of the Q-switched TDFL as a function of launched pump power. Inset shows the single pulse shape at 2.43 W output level. Dots are measured data, and all lines are just for guiding the eye.
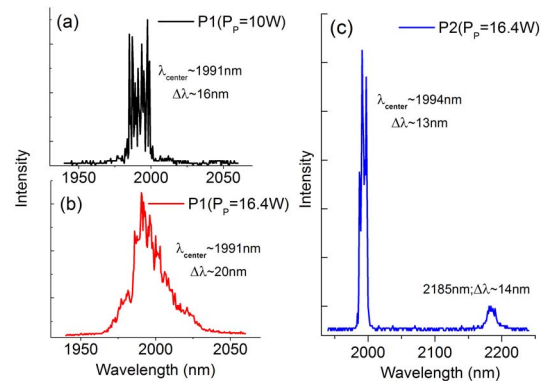
Fig. 5. Laser spectra of the Q-switched TDFL from fiber ends P1 (a) and (b) and P2 (c) at two pump levels of 10 and 16.4 W.

Stokes peak appears at 2185 nm with a bandwidth of ~14 nm. This Raman peak can be employed to construct a pulsed Raman fiber laser with the present system configuration slightly modified.

The output beam quality is determined by the signal fiber of the combiner, which has a 10 μm (NA = 0.15) core, giving a normalized frequency of ~2.343, less than the single-mode condition of $V = 2.4048$. This guarantees the fiber laser operating in the fundamental-mode situation.

In conclusion, a high-power 2 μm TDFL passively Q-switched by using strong randomly distributed SBS from a piece of high nonlinear fiber is reported for the first time. This new kind of Q-switching technique can provide tens of kHz RR, ~50 μJ pulse energy and >2 W average power, all of which are comparable to those of positively Q-switched fiber lasers. In addition, this fiber laser has a simple all-fiber configuration with low cost, which is difficult to be realized with positively modulating techniques currently. This novel Q-switching approach also can be extended to other rare earth (Er^{3+}, Yb^{3+}, etc.)-doped fibers; thus it opens a new way to achieve pulsed fiber lasers by harnessing nonlinear effects. We can expect that, in the near future, a single specially designed gain fiber with high nonlinearity (or through special configuration design or special doping profile) will provide pulsing operation without the requirement of any modulators. Acting as a seed source, this kind of high-power pulsed fiber laser will greatly simplify the MOPA fiber system.

References

1. Y. Zhang, Y. Tian, W. Wang, and B. Yao, Laser Phys. Lett. **7**, 225 (2010).
2. F. Wang, D. Y. Shen, D. Y. Fan, and Q. S. Lu, Laser Phys. Lett. **7**, 450 (2010).
3. C. C. C. Willis, E. McKee, P. Boswetter, A. Sincore, J. Thomas, C. Voigtlander, R. G. Kramer, J. D. Bradford, L. Shah, S. Nolte, A. Tunnermann, and M. Richardson, Opt. Express **21**, 10467 (2013).
4. http://www.qpeak.com/Aboutus/news.shtml.
5. A. F. El-Sherif and T. A. King, Opt. Lett. **28**, 22 (2003).
6. Y. Tang, Y. Yang, J. Xu, and Y. Hang, Opt. Commun. **281**, 5588 (2008).
7. R. C. Sharp, D. E. Spock, N. Pan, and J. Elliot, Opt. Lett. **21**, 881 (1996).
8. M. A. Solodyankin, E. D. Obraztsova, A. S. Lobach, A. I. Chernov, A. V. Tausenev, V. I. Konov, and E. M. Dianov, Opt. Lett. **33**, 1336 (2008).
9. M. Eichhorn and S. D. Jackson, Opt. Lett. **32**, 2780 (2007).
10. F. Stutzki, F. Jansen, C. Jauregui, J. Limpert, and A. Tunnermann, Opt. Lett. **38**, 97 (2013).
11. Y. J. Zhang, B. Q. Yao, Y. L. Ju, and Y. Z. Wang, Opt. Express **13**, 1085 (2005).
12. B. C. Dickinson, S. D. Jackson, and T. A. King, Opt. Commun. **182**, 199 (2000).
13. Y. Tang and J. Xu, Appl. Phys. Express **5**, 072702 (2012).
14. Y. L. Tang, L. Xu, Y. Yang, and J. Q. Xu, Opt. Express **18**, 22964 (2010).
15. M. Jiang and P. Tayebati, Opt. Lett. **32**, 1797 (2007).
16. N. Simakov, A. Hemming, S. Bennetts, and J. Haub, Opt. Express **19**, 14949 (2011).
17. M. Eichhorn, Opt. Lett. **30**, 3329 (2005).
18. A. M. Heidt, Z. Li, J. Sahu, P. C. Shardlow, M. Becker, M. Rothhardt, M. Ibsen, R. Phelan, B. Kelly, S. U. Alam, and D. J. Richardson, Opt. Lett. **38**, 1615 (2013).
19. W. Shi, E. B. Petersen, D. T. Nguyen, Z. Yao, A. C. Pirson, N. Peyghambarian, and J. Yu, Opt. Lett. **36**, 3575 (2011).
20. Q. Wang, J. Geng, T. Luo, and S. Jiang, Proc. SPIE **8237**, 82371W (2012).
21. Z. J. Chen, A. B. Grudinin, J. Porta, and J. D. Minelly, Opt. Lett. **23**, 454 (1998).
22. M. Laroche, H. Gilles, and S. Girard, Opt. Lett. **36**, 241 (2011).
23. A. A. Fotiadi, P. Megret, and M. Blondel, Opt. Lett. **29**, 1078 (2004).
24. S. V. Chernikov, Y. Zhu, J. R. Taylor, and V. P. Gapontsev, Opt. Lett. **22**, 298 (1997).
25. A. A. Fotiadi and P. Megret, Opt. Lett. **31**, 1621 (2006).
26. S. K. Turitsyn, S. A. Babin, A. E. El-Taher, P. Harper, D. V. Churkin, S. I. Kablukov, J. D. Ania-Castanon, V. Karalekas, and E. V. Podivilov, Nat. Photonics **4**, 231 (2010).
27. G. P. Agrawal, *Nonlinear Fiber Optics*, 4th ed. (Academic, Elsevier, 2007).
28. F. Z. Qamar and T. A. King, Opt. Commun. **248**, 501 (2005).
29. S. D. Jackson, Appl. Opt. **46**, 3311 (2007).
30. G. P. Agrawal, *Nonlinear Fiber Optics*, 4th ed. (Academic, Elsevier, 2007), p. 330.
31. Y. L. Tang, J. Q. Xu, W. Chen, and S. Y. Li, Chin. Phys. Lett. **27**, 104207 (2010).